IEEE Access
Multidisciplinary | Rapid Review | Open Access Journal

Received 7 April 2025, accepted 23 April 2025, date of publication 2 May 2025, date of current version 13 May 2025.

*Digital Object Identifier 10.1109/ACCESS.2025.3566446*

RESEARCH ARTICLE

# Experimental 5G Network Performance Analysis in a Semi-Anechoic and Semi-Reverberation Chamber

**FELIX DELGADO-FERRO[1], ALEJANDRO RAMÍREZ-ARROYO[2], JORGE NAVARRO-ORTIZ[1], AND JUAN F. VALENZUELA-VALDÉS[1]**

[1]Department of Signal Theory, Telematics and Communications, Research Centre for Information and Communication Technologies (CITIC-UGR), University of Granada, 18014 Granada, Spain
[2]Department of Electronic Systems, Aalborg University (AAU), 9220 Aalborg, Denmark

Corresponding author: Felix Delgado-Ferro (felixdelgado@ugr.es)

This work was supported in part by Spanish Ministry of Science and Innovation funded by MICIU/AEI/10.13039/501100011033 and ERDF/EU under Grant PID2022-137329OB-C43; in part by Spanish Ministry for Digital Transformation and Civil Service funded by European Union through the Recovery, Transformation and Resilience Plan–NextGenerationEU under Grant TSI-063000-2021-28/6G-CHRONOS; and in part by Spanish Ministry of Universities under Grant FPU20/02621.

**ABSTRACT** 5G New Radio wireless networks based on the International Mobile Telecommunications specifications are fundamental for current mobile communications. This work focuses on the performance analysis of a private 5G network in an experimental and controlled environment. For this purpose, exhaustive experimentation considering 192 combinations of factors has been proposed and carried out in a controlled environment within a semi-anechoic and semi-reverberant chamber. This enables accurate observation of the impact of the studied factors on a series of Key Performance Indicators that are fundamental in 5G networks, such as latency, throughput, and reliability. This dataset has been analyzed using statistical algorithms such as Principal Component Analysis and SHapley Additive exPlanations. The results show how network performance can be affected not only by the environment, but also by its configuration. Furthermore, the configurations contribute differently depending on the indicator, showing that these can be improved without an excessive impact on other indicators: (i) throughput improves by more than 26% by modifying parameters such as bandwidth, duplexing method, or number of antennas; (ii) latency improves over 7% by modifying the duplexing method or 12% by switching between radio access technologies; (iii) reliability is exceptionally high in controlled environments. Our study shows that reliability can achieve improvements of up to 196.5% in terms of lost and retransmitted packets. The insights found in this work, based on the proposed configurations and their respective improvements, can be extrapolated to proposed use cases for 5G networks.

**INDEX TERMS** 5G network, 5G performance, anechoic chamber, feature importance analysis, multivariate exploratory data analysis, new radio, principal component analysis, reverberation chamber.

## I. INTRODUCTION

The exponential growth of wireless networks in recent decades has driven the need for advancements in mobile communications. This demand will be met by the fifth generation (5G) of mobile networks [1], [2]. In recent years, studies have analyzed the requirements of this technological evolution [3], leading to the definition of expected 5G New Radio (NR) specifications under International Mobile Telecommunications-2020 (IMT-2020). Three key service categories have been established: Enhanced Mobile Broadband (eMBB), Ultra Reliable Low Latency Communications (URLLC), and Massive Machine Type Communications (mMTC) [4]. Our work focuses on eMBB and URLLC, which are described as:

- **Enhanced Mobile Broadband:** Designed to significantly increase the user data rate, reaching tens of Gbps, while reducing latency to 4 ms [4]. Key applications

The associate editor coordinating the review of this manuscript and approving it for publication was Ronald Chang.

© 2025 The Authors. This work is licensed under a Creative Commons Attribution 4.0 License.
For more information, see https://creativecommons.org/licenses/by/4.0/

include virtual and augmented reality [5], [6], [7], cloud computing [8], [9], [10] or holographic video streaming [11], [12].

- **Ultra Reliable Low Latency Communications:** Aimed at scenarios requiring extremely low latency and high service availability, with expected throughput of 100 Mbps per user and end-to-end latency below 1 ms [4]. These requirements can be met using paradigms such as Edge Computing or Fog Computing [13]. Typical applications include industrial automation [14], [15], [16] and self-driving smart cars [17], [18].

Several theoretical 5G use cases are outlined in the Technical Specifications (TS) of 3GPP [19], [20], [21]. However, most remain unassessed due to the high economic and time costs associated with real-world deployment, experimentation, and analysis. Our work provides an overview not only of the Quality of Service (QoS) in a private 5G network deployment but also of 3GPP use cases that can be effectively supported.

Evaluating 5G networks performance poses significant technological challenges, particularly when analyzing 192 different variable combinations. This study was conducted in a controlled environment —specifically a semi-anechoic and semi-reverberant chamber—, eliminating external environment factors that could affect measurements in a commercial network. The use of private networks in controlled environments allows a general validation of devices or standards under study, which will later be particularized to specific use cases given experimentation in real-world scenarios. Additionally, the proposed setup and methodology ensure the reproducibility of results independently of external effects, ensuring accurate and reliable assessment of Key Performance Indicators (KPIs). A private 5G network was deployed using Amarisoft [22] and a smartphone to capture the respective KPI measurements. Given the growing relevance of private networks in industry, business, utilities, and the public sector –along with their technical and implementation challenges [23]– this study is particularly significant.

In summary, the key contributions of this paper are detailed below:

1) This paper presents an experimental 5G testbed and details a comprehensive exhaustive experimental methodology. A key contribution is the deployment of a private 5G network within a semi-anechoic and semi-reverberant chamber, ensuring precise measurements free from external unknown interferences. By thoroughly detailing the experimental setup and methodology, this study provides a robust replicable framework, enhancing result reliability and serving as a benchmark or baseline for future research on 5G deployment and optimization.
2) The collected measurements offer an empirical assessment of current 5G communication capabilities based on the 3GPP Release 16 implementation [24], evaluating throughput, latency, and reliability in a controlled private scenario. These results form a dataset covering 192 tested configurations, which can support both Mobile Network Operators (MNOs) and the research community, particularly in deterministic 5G modeling [25], [26]. To promote research dissemination, our dataset is publicly available via GitHub at [27].
3) 5G performance exhaustive analysis is conducted using the dataset, comparing QoS requirements (throughput, latency, and reliability) across multiple factor combinations, including radio access technology, duplex mode, bandwidth, number of antennas, chamber area, and antenna polarization. This analysis consists of:
   - **Multivariable performance analysis:** applies Principal Component Analysis (PCA) [28] to assess KPI trade-off across all variables.
   - **Univariate performance analysis:** employs SHapley Additive exPlanations (SHAP) [29] to evaluate the impact of the most relevant variables on each KPI.
4) Finally, this study identifies and evaluates eMBB and URLLC use cases that can be supported by the current 5G network (Rel. 16). By analyzing network configurations and their impact on these services, it provides valuable insights into the key parameters required to meet the strict demands of advanced applications.

This paper is structured as follows. Section II presents related work, comparing recent studies on 5G real-world measurements. Section III explains the experimental setup and design of experiments, highlighting key variables and KPIs (throughput, latency, and reliability). Section IV discusses 5G NR network performance, providing comparisons and a brief evaluation of eMBB and URLLC use cases under similar network configurations. Finally, Section V summarizes the main conclusions and outlines potential directions for future research.

## II. RELATED WORK

5G technology marks a major advancement in telecommunications, promising unprecedented data rates, low latency, and robust connectivity simultaneously [30], [31], [32]. However, achieving these stringent requirements is challenging due to several technical and operational complexities. The key issues include:

- **Challenges of private 5G deployment:** The literature highlights several challenges in implementing and experimenting with 5G networks, extending beyond technical, economic, and logistical aspects. Deploying an experimental 5G network that captures multiple scenarios is complex due to the numerous internal and external parameters affecting performance [33], [34], [35]. For instance, the Radio Access Network (RAN) can operate across multiple frequency bands, primarily

licensed bands in Frequency Range 1 (FR1) (Sub-6 GHz) or Frequency Range 2 (FR2) (mmWave), typically managed by mobile operators [36], [37]. Consequently, most real-world experiments rely on commercial infrastructure, as seen in [36], [38], and [39]. In contrast, our study employs a private indoor deployment within a semi-anechoic and semi-reverberation chamber to avoid external disturbances such as electromagnetic interference, obstructions, and environmental conditions. This controlled setting ensures accurate measurements and isolates the impact of the selected parameters, and they have been widely employed for 5G antenna design validation, Over-the-Air 5G device testing, or radio-propagation studies [40], [41], [42], [43], [44], [45].

Moreover, deploying private 5G infrastructure incurs substantial costs due to specialized hardware and software requirements [34], [35], [38]. It also demands significant time for implementation and experimentation, along with expenses for skilled personnel required for deployment, configuration, metric collection, and analysis [33].

- **Empirical experimentation and analysis:** The selection of KPIs is crucial for evaluating 5G networks performance. According to 3GPP [46] and the previous studies [34], [36], [38], [47], [48], KPIs include data bitrate, latency, reliability, and coverage. Our work focuses on the first three indicators.

  Beyond deployment, 5G networks present challenges in parametrization and measurement accuracy [33], [34], [49], [50]. Achieving precise measurements requires advanced methodology, as the outdoor environment introduces uncontrolled factors such as reflections and obstructions [33], [49]. To mitigate these issues, our work employs a semi-anechoic and semi-reverberant chamber, ensuring controlled conditions and reliable data collection.

  Measurement challenges in 5G networks arise from their complexity and limited access to detailed information from the User Equipment (UE) and network infrastructure [47]. Additionally, variations in measurement tools [34] and ongoing network evolution [34], [47], [48] hinder reproducibility and result comparison. Works [34], [39], [51] highlight the trade-off between KPIs, where improving one metric can negatively affect others.

  Most prior works as [32], [34], [36], [38], [39], [47], [48], [49], [52], and [53] employ univariate analyses, limiting the understanding of KPI interdependencies. In contrast, our work presents both univariate and multivariate analyses, evaluating 192 different configurations. A PCA approach is introduced to clarify the trade-off between throughput, latency, and reliability. These analyses enable optimized network configuration and resource allocation.

- **Study of the use case requirements:** 5G experimentation focuses on meeting the requirements of advanced services such as eMBB and URLLC [50]. Our work evaluates the current state of private 5G networks through a case study analyzing use cases of these services.

This work brings together the three previous concepts, thus proposing a setup that allows to empirically evaluate various KPIs in 5G networks through the deployment of a private network in a controlled environment such as a semi-anechoic and semi-reverberant chamber. This deployment allows the reproducibility of tests in laboratory environments without external interferences caused by other devices, as it might occur in a public commercial network. Thus, Table 1 provides a comprehensive comparison between our work and the state-of-the-art, summarizing RAN technologies, 3GPP releases, services, KPIs, among other properties.

## III. METHODOLOGY

This section outlines the methodology used in this work. First, it describes the experimental environment, detailing the setup where the experiments were conducted. Second, it presents the experimental design, specifying the selected variables and KPIs.

### A. EXPERIMENTAL SETUP

#### 1) CHAMBER ENVIRONMENT

This work analyzes 5G network performance in controlled scenarios. The testbed scenario consists of a semi-anechoic and semi-reverberation chamber measuring 5 × 3.5 × 3.5 meters (61.25 $m^3$). Acting as a Faraday cage, the chamber eliminates external electromagnetic interference or degradation by obstructions, ensuring that all observed electromagnetic phenomena generate within the setup. It allows for the real and precise assessment of the impact of variables on the KPIs.

The semi-anechoic section ensures a Line-of-Sight (LoS) propagation channel between the transmitter (Tx) and receiver (Rx) by attenuating reflections with absorbers on the wall (see Fig. 1(a)). In contrast, when Tx is points toward the semi-reverberation section, the metallic walls (see Fig. 1(a)) induce multiple reflections, creating a strong multipath effect. These controlled configurations allow for a detailed analysis of multiple mobile network performance scenarios.

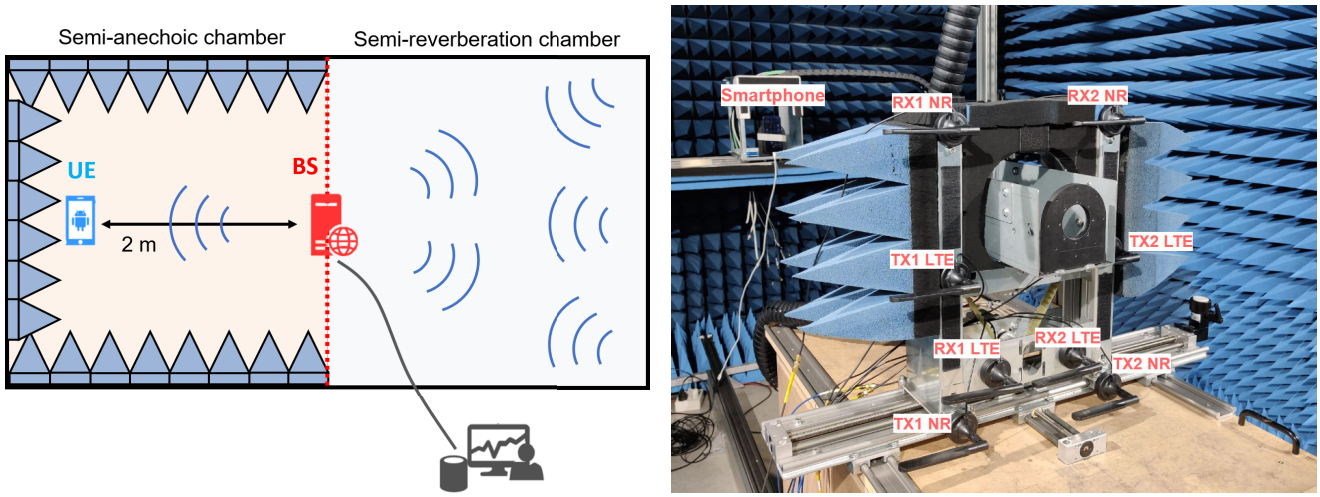
#### 2) 5G TESTBED

The 5G system consists of a 5G base station and a Huawei P40 smartphone (see Fig. 1(b)).

The base station is implemented on a Supermicro SYS-7049P-TRT running Ubuntu Server 18.04, hosting the Amarisoft 5G Core Network (5G-CN). The 5G-RAN operates with two AD9361-based PCIe SDRs, supporting up to eight antennas (four Tx and four Rx) and providing a transmission power of 20 dBm within the 1800-2600 MHz frequency bands. The system operates in Frequency Division

**TABLE 1. Comparison with recent works on 5G performance.**

| Property | [38] | [52] | [36] | [47] | [49] | [32] | [34] | [48] | [39] | Our work |
|---|---|---|---|---|---|---|---|---|---|---|
| Year | 2020 | 2020 | 2021 | 2021 | 2022 | 2023 | 2023 | 2023 | 2024 | |
| Network | Public | Sim. | Private | Public | Public | Public | Public | Public | Public | Private |
| Scenario | Open net | - | Controlled | Open net | Open net | Open net | Open net | Open net | Open net | Controlled |
| RAN Tech. | 4G/5G | 5G | 5G | 4G/5G | 5G | 5G | 4G/5G | 5G | 5G | **4G/5G** |
| 3GPP Release | Rel-15 | Rel-16 | Rel-15 | - | - | Rel-16 | Rel-15 | - | Rel-15 | **Rel-16** |
| 5G Frequency | FR1 | FR1/FR2 | FR1 | FR1/FR2 | FR1/FR2 | FR1/FR2 | FR1/FR2 | FR1 | FR1/FR2 | **FR1** |
| 5G Services | - | URLLC | - | - | - | V2X | - | - | - | **eMBB/URLLC** |
| Analysis | Univ. | Univ. | Univ. | Univ. | Univ. | Univ. | Univ. | Univ. | Univ. | **Univ./Multiv.** |
| Throughput | ✓ | ✓ | ✗ | ✓ | ✓ | ✓ | ✓ | ✗ | ✓ | ✓ |
| Latency | ✓ | ✓ | ✓ | ✗ | ✓ | ✗ | ✓ | ✓ | ✓ | ✓ |
| Reliability | ✗ | ✓ | ✓ | ✗ | ✗ | ✗ | ✗ | ✗ | ✗ | ✓ |
| Coverage | ✓ | ✓ | ✗ | ✓ | ✗ | ✓ | ✓ | ✓ | ✓ | ✗ |
| Dataset | ✓ | ✗ | ✓ | ✗ | ✗ | ✗ | ✗ | ✗ | ✓ | ✓ |




(a) (b)

**FIGURE 1. Experimental setup of 5G performance. (a) The drawing shows the schematic of the complete experimental setup with the reflections that can occur in each chamber area. (b) The photo shows the 5G NR base station and smartphone oriented to the semi-reverberant area. It also shows the arrangement of the base station antennas with sufficient distance to avoid electromagnetic interference.**

Duplex (FDD) mode on Band 1, with a central frequency of 2140 MHz, and in Time Division Duplex (TDD) mode on Band 38, with a central frequency of 2570 MHz. The linear polarized antennas operate in 700 MHz - 6 GHz (Sub-6GHz) band with a 5 dBi gain. These antennas are strategically placed $\lambda/2$ to prevent frequency hopping.

The UE (smartphone) operates with a transmission power of 15 dBm and is positioned 200 cm from the base station at a height of 130 cm, while the base station antennas are mounted at heights between 94 cm and 128 cm. The nearest wall is 175 cm away. An external computer manages, monitors, and stores the experimental data, ensuring accurate and reliable 5G performance metrics.

### B. DESIGN OF EXPERIMENTS

The experimental design is pivotal in assessing the 5G network performance, involving measurement tools, QoS KPIs, and configuration variables to analyze their impact.

To collect data, iperf3 and ping are employed. Iperf3 generates Transmission Control Protocol (TCP) traffic with 20 parallel flows to measure throughput. Ping measures Round Trip Time (RTT) to compute network latency.

To minimize the randomization of results, ensuring result reliability, measurements are repeated 20 times at different intervals. In addition, to prevent configuration errors, connection disruptions, or manual mistakes, the experiment procedures are automated (see Fig. 2).

The measured KPIs in these experiments focus on throughput, latency, and reliability. The dataset includes all metrics provided by the measurement tools, which are used in the multivariable performance analysis. These metrics include byte transfer [Bytes], throughput [bits/s], retransmitted packets rate, Internet Control Message Protocol (ICMP) Time [ms], minimum RTT [ms], Average RTT [ms], Maximum RTT [ms], Standard Deviation Round Trip Time [ms].

For univariate performance analysis, the study focuses on the main KPIs:

- **Throughput:** measures the average data rate successfully transmitted over a time slot. The maximum theoretical throughput in our testbed is 200 Mbps due to software license and hardware limitations.

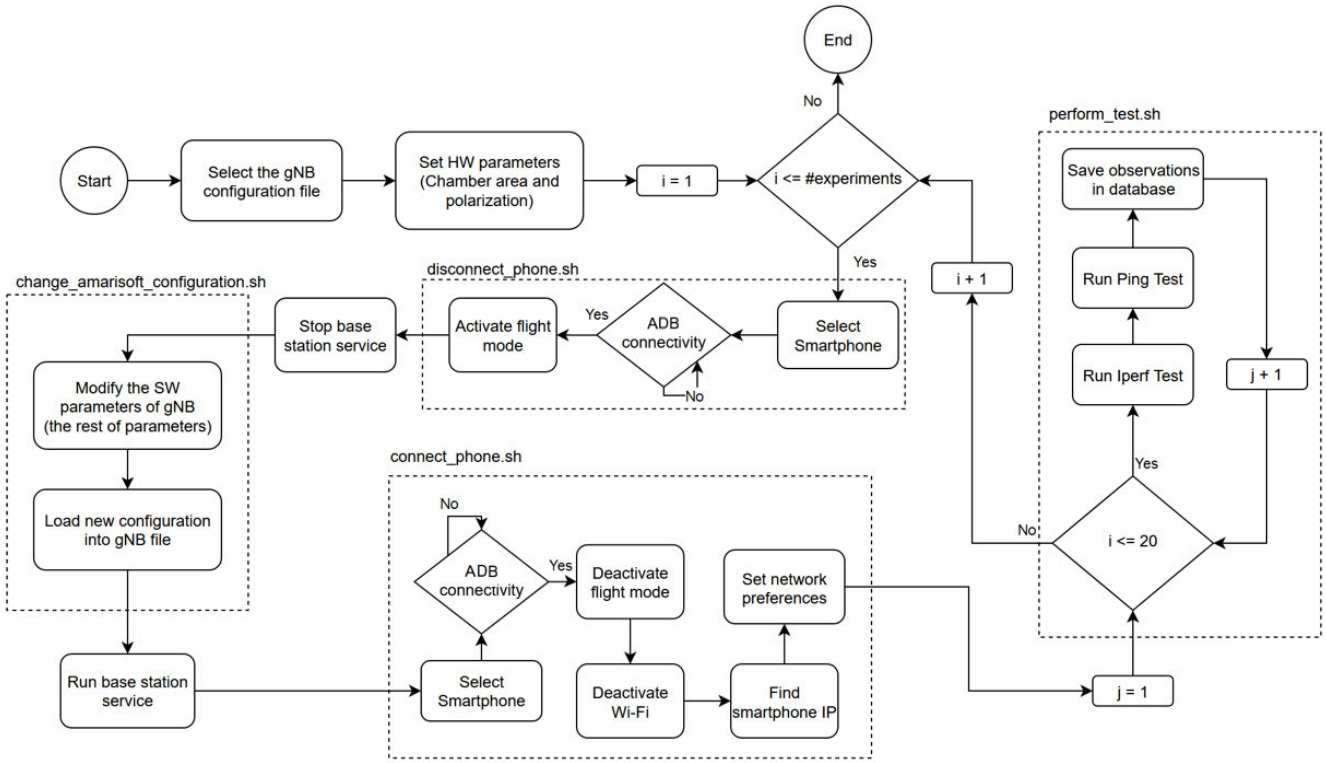



**FIGURE 2.** Experimental automatization of 5G campaign.

**TABLE 2.** Summary of experimental variables of configuration.

| Variable | Acronym | Values |
|---|---|---|
| RAN Technology | Tech | 4G LTE / 5G NR |
| Duplex mode | Duplex | FDD (band 1) / TDD (band 38) |
| Bandwidth | BW | 5 / 10 / 15 /20 MHz |
| Number of antennas | N_Ant | SISO / MIMO 2x2 |
| Chamber area | Chamber | Anechoic / Rever |
| Antenna polarization | Polarization | Vertical (V) / Horizontal (H) / Pointing (P) |

- **Latency:** represents the total signal transmission time, including initial transmission, processing at the destination, and acknowledgment return.
- **Reliability:** evaluated through the retransmitted packets rate, which indicates network congestion or errors based on the number of packets retransmitted within a specific time interval.

The experiments are exhaustively conducted under multiple software and hardware configurations, systematically modifying key variables to assess their impact on 5G performance. These variables are summarized in Table 2 and described below.

1) **Radio access technologies:** This parameter distinguishes between LTE and NR technologies. LTE serves as a baseline comparison, allowing a useful evaluation of improvements introduced by NR. Comparing both under identical conditions helps identify whether observed performance gains are due to network architecture improvements or other factors [54], [55].
2) **Duplex mode:** communication can occur using Frequency Duplexing Division or Time Duplexing Division. Studying both helps to analyze differences in spectrum efficiency, interference handling, and real performance.
3) **Bandwidth:** it refers to width of the allocated spectrum, which influences data capacity and transmission efficiency. Four different bandwidths are tested to assess how network performance scales with higher spectrum allocation. This is crucial since real-world 5G deployments often vary in terms of available spectrum – spectrum is oversaturated.
4) **Number of antennas:** configurations include ''Single Input, Single Output'' (SISO) or ''Multiple Input, Multiple Output'' (MIMO). In this study, the cell was deployed using a single SDR, which limits the available MIMO configuration to MIMO $2 \times 2$. Evaluating both SISO and MIMO highlights the impact of multiple antennas in controlled environments, particularly in private 5G setups where hardware constraints may influence performance.
5) **Chamber area:** it means the area of the chamber where the transmission takes place, classified into anechoic area (with LoS propagation) and reverberant area (with multipath effect). Comparing both allows

assessment of 5G's resilience to real-world interference and channel variations.

6) **Antenna polarization:** it is the orientation of the antennas relative to the receiver, classified as vertical (V), horizontal (H), or pointing towards the receiver (P). Antenna polarization mismatch can lead to signal degradation and reduced performance. Testing these configurations provides valuable insights into optimal antenna polarization for a private 5G network.

This study considers six parameter modifications, leading to a total 192 possible variable combinations, calculated as ($2 \times$ Tech $+ 2 \times$ Duplex $+ 4 \times$ BW $+ 2 \times N_{\text{ant}} + 2 \times$ Chamber $+ 3 \times$ Polarization). For instance, one combination could be NR, FDD, 20 MHz, MIMO 2×2, Anechoic, Vertical; while another could be NR, TDD, 10 MHz, MIMO $2 \times 2$, Reverberation, Pointing.

## IV. PERFORMANCE ANALYSIS

The analysis is based on measurements from all variable combinations. First, Multivariate Exploratory Data Analysis (MEDA) is applied using PCA [28] to understand KPI interactions. Then, a univariate performance analysis is conducted using Feature Importance (FI) techniques such as SHAP [29], regression methods and Cumulative Distribution Function (CDF) analysis. Based on these results, radio access technologies (LTE and NR) are compared across four combinations: the optimal configurations for throughput, latency, and reliability; as well as a balanced trade-off among KPIs. These optimal configurations are established through the previous analyses. Additionally, ten use cases for eMBB and URLLC services are analyzed to determine suitable configurations for meeting QoS requirements.

To facilitate the understanding of the mathematical expressions presented in this section, Table 3 summarizes the main notations and operators used throughout the analysis.

### A. MULTIVARIATE PERFORMANCE ANALYSIS

Multivariate Exploratory Data Analysis aims to understand relationships between different indicators. PCA identifies linear patterns in KPI behavior relative to initially uncorrelated configurations. This statistical analysis reduces dimensionality by transforming original variables into principal components (PCs) while preserving maximum data variability. It also simplifies our model and removes redundancy. PCA applies these processes [28]:

1) **Normalization of Principal Components:** assuming a dataset ($X$) with number of observation ($N_o$) and KPIs ($P$), where each observation is represented as $X_n = X_1, X_2, \ldots, X_P, \forall n \in [1, N_o]$. The data is normalized by centering each KPI (subtracting its mean ($\bar{X}$)) and scaling by its standard deviation ($\sigma_x$). This ensures that all KPIs – which have different units – are comparable. The normalized matrix ($\dot{X}$) is calculated by (1). After normalization, Principal Components ($K$) are computed according to (2).

$$\dot{X} = \frac{X - \bar{X}}{\sigma_x} \tag{1}$$

$$Z_k = \sum_{j=1}^{P} \phi_{jk} \dot{X}_j \tag{2}$$

where $Z_k$ is the projection of the data onto the $k_{th}$ principal components, $K$ denotes principal component, $\phi_{jk}$ is the loading of KPI ($X_j$) in the $k_{th}$ principal component, indicating its contribution to the new dimension, and $\dot{X}_j$ represents the normalized KPI $j$.

2) **Covariance matrix, eigenvalues, and eigenvectors:** the covariance matrix of the normalized data ($C$) is calculated as (3).

$$C = \frac{1}{N_o} Z^T Z = \frac{1}{N_o} \sum_j \lambda_j v_j v_j^T \tag{3}$$

where the matrix of projections ($Z$) represents all the selected principal components for all observations, the matrix $Z^T$ is its transpose matrix, the eigenvalues $\lambda_j$ provide a measure of the variance captured by each principal component, and eigenvector $v_j$ define the direction of these components in the feature space.

Before applying Principal Component Analysis, it is essential to determine the optimal number of principal components ($K$) that retain meaningful information. This is achieved by analyzing residual variance and performing cross-validation, as illustrated in Fig. 3.

The appropriate $K$ is identified at the breakpoint where residual variance concerning cross-validation stabilizes.

**TABLE 3. Summary of notations and operators.**

| Notation | Description |
|---|---|
| $X$ | Matrix with configurations, KPIs and observations |
| $N_o$ | Number of observations |
| $P$ | Key Performance Indicators |
| $\bar{X}$ | Mean value of each KPI across all observations |
| $\sigma_x$ | Standard deviation of each KPI |
| $\dot{X}$ | Normalized dataset matrix |
| $K$ | Number of principal components retained after PCA |
| $Z_k$ | Projection of the data on $K_{th}$ principal component |
| $\phi_{jk}$ | Loading factor of KPI $X_j$ in $K_{th}$ principal component |
| $\dot{X}_j$ | Normalized KPI $j$ |
| $C$ | Covariance matrix of the normalized dataset |
| $Z$ | Matrix of projections of observations |
| $Z_T$ | Transpose of the projection matrix $Z$ |
| $\lambda_j$ | Eigenvalue $j$, variance explained by each component |
| $v_j$ | Eigenvector $j$, direction of the principal component |
| $d$ | Dummy variable for oMEDA analysis |
| $d^2_{A,(p)}$ | Quadratic index for KPI in PC space |
| $\Sigma^d_{(p)}$ | Weighted sum of elements in indicator for dataset |
| $\Sigma^d_{A,(p)}$ | Weighted sum of elements in indicator for subset $A$ |
| $\gamma_j$ | Shapley value (average marginal contribution) for $j$ |
| $N_c$ | Set of all configurations |
| $S$ | Subset (coalition) of configurations containing $j$ |
| $f(S)$ | Output when using configuration subset $S$ |
| $[f(S) - f(S \setminus j)]$ | Output when remove configuration $j$ from subset $S$ |

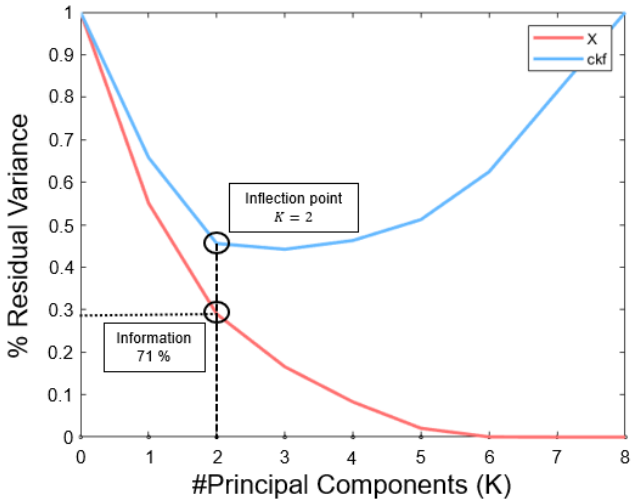



**FIGURE 3.** Residual variance of the dataset for different numbers of principal components in PCA. The red line (X) represents the residual variance after dimensionality reduction, while the blue line (ckf) depicts the cross-validation results obtained using the columnwise k-fold algorithm [57].

In this study, this occurs at $K = 2$, where cross-validation indicates an inflection point and the residual variance falls below 30%. Consequently, two principal components are used, representing 71% of the dataset total variability and reducing dimensionality from eight to two indicators.

Subsequently, the loadings of each KPI are estimated via PCA. Fig. 4(a) shows the distribution of KPIs as a function of two PCs. This graph suggests two dominant trends. The first – indicated by the green arrow – aligns with increasing throughput and retransmissions. The second – shown by the blue arrow – corresponds to the dispersion of observations along transmission time, particularly $\text{RTT}_{\text{avg}}$ and $\text{RTT}_{\text{max}}$. These trends are orthogonal in the two-component representation, suggesting that KPIs are uncorrelated – changes in transmission time do not necessarily affect throughput or another KPI. In other words, they are uncorrelated. In addition, the observations result from the combined influence of multiple KPIs.

Fig. 4(b) illustrates the distribution of observations projected onto the two principal components, categorized by bandwidth. As the bandwidth increases, the distribution shifts significantly, following the first trend (green arrow) associated with higher throughput. Additionally, a more gradual shift toward latency is observed, aligning with the second trend (blue arrow). This implies that different configurations influence the KPIs, making it feasible to establish a trade-off between them.

Fig. 4(c) compares clusters (5 MHz and 20 MHz observations) using observation-based Multivariate Exploratory Data Analysis (oMEDA) [58]. This algorithm categorizes the observations into clusters, trends, or outliers; and applies Multivariate Statistical Process Control (MSPC). The MSPC assesses KPI contributions by creating subset variables corresponding to KPI subspaces. A dummy variable ($d$) is introduced to independently identify observations in each subset. The relationship among subsets is determined through contribution weights, quantified by quadratic indices ($d^2_{A,(p)}$) defined in (4) [59]:

$$d^2_{A,(p)} = \frac{1}{N_o}\left(2\Sigma^d_{(p)} - \Sigma^d_{A,(p)}\right)|\Sigma^d_{A,(p)}| \tag{4}$$

where $N_o$ is the total number of observations, $P$ represents KPIs, $\Sigma^d_{(p)}$ and $\Sigma^d_{A,(p)}$ denote the weighted sum of elements for the indicator $p$ in the dataset and its projection ($A$) according to the weights ($d$), respectively. In this context, the weights indicate that bandwidth significantly influences throughput indicators while having a more subtle impact on packet retransmission rate and latency.

Thus, the two hypothesized trends are confirmed as statistically robust. The first trend is the most dominant, while the second remains significant. All KPIs are influenced by the observations as discussed above.

### B. UNIVARIATE PERFORMANCE ANALYSIS

Univariate analysis offers a deeper understanding of performance metrics. Multivariate analysis determines that all KPIs are influenced by configuration parameters. Fig. 4(d) shows the correlation matrix of the KPIs. It reveals a strong correlation between byte transfer and throughput, while retransmitted packets exhibit a slight correlation with both. RTT metrics are also highly correlated, except for $\text{RTT}_{\text{min}}$. To simplify the analysis, a selection method based on correlations is applied, resulting in the choice of three KPIs: throughput, $\text{RTT}_{\text{avg}}$ for latency, and retransmitted packets for reliability.

These KPIs are weakly correlated with each other and provide meaningful insights. Throughput shows the amount of information successfully transmitted and is essential for eMBB. Latency, measured via RTT, is crucial for URLLC services. In our tests, latency is defined as the one-way transmission time between the base station and the smartphone, approximated as half of RTT. Reliability is a relevant metric for understanding the network performance, especially for URLLC services aiming for minimal packet loss and consistent transmission. While packet loss rate (%) is typically used to evaluate reliability, our observations show minimal losses due to controlled radio conditions in a semi-anechoic and semi-reverberant chamber. Given the short antenna distances at the tested frequencies, reliability is assumed to be extremely high. Instead of packet loss rate, reliability is analyzed using the retransmitted packets rate (%).

Firstly, we consider that different configurations have varying contributions to the KPIs, as predicted by the multivariate analysis. To quantify this contribution, the SHAP algorithm [60] is applied to each selected KPI. This method provides an intuitive and interpretable visualization of the results by illustrating each configuration on the KPI outcome.

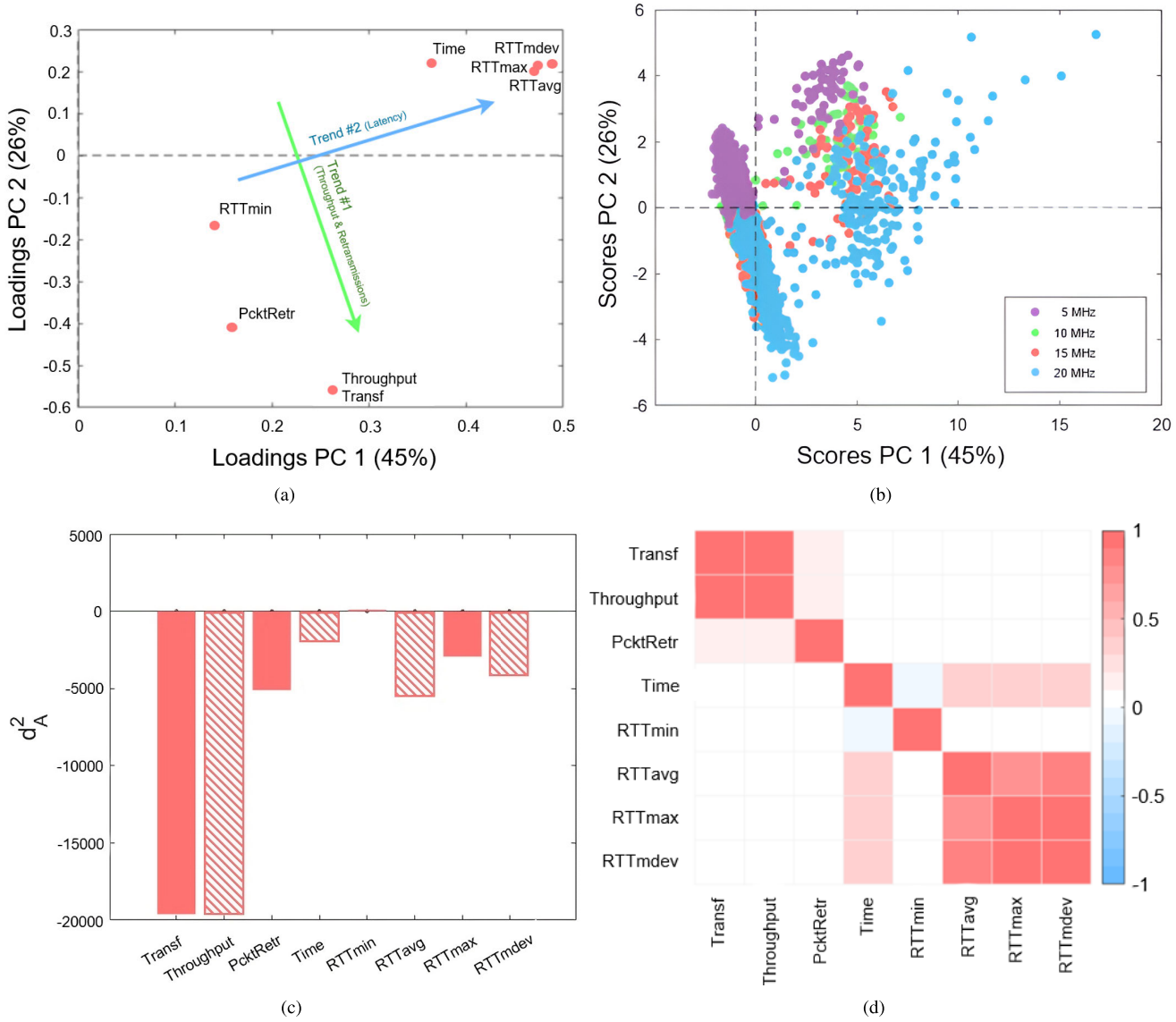



**FIGURE 4.** Two-principal-component PCA on bandwidth-ranked observations. (a) Loading Distribution of KPIs on two-component analysis. (b) Distribution of bandwidth-ranked observations. (c) Comparison via oMEDA between 5 MHz and 20 MHz observations. (d) Correlation matrix between KPIs.

SHAP, a game-theoretic approach, explains statistical model outcomes by linking optimal feature allocation to local explanations using Shapley values. The Shapley values are computed using (5) [61]:

$$\gamma_j = \sum_{S \subseteq N_c, j \in S} \frac{(|S|-1)!(|N_c|-|S|)!}{|N_c|!} [f(S) - f(S \setminus j)] \quad (5)$$

where $\gamma_j$ represents the Shapley value assigned to each configuration ($j$), representing its average marginal contributions to the KPI. $N_c$ is the set of all configurations analyzed, $S \subseteq N_c$ represents a subset (coalition) of configuration, where $j$ belongs to $S$. $|S|$ and $|N_c|$ are the number of configurations in subset $S$ and in the full set $N_c$, respectively. $f(S)$ is the model function evaluating the KPI outcome when using the subset ($S$). $f(S \setminus j)$ is the KPI outcome when removing configuration $j$ from subset $S$. Then, the term $[f(S) - f(S \setminus j)]$ represents the marginal contributions of configuration $j$ to subset $S$. The equation considers all possible subsets $S$ where $j$ is present, ensuring a fair distribution of contributions across different configurations.

Performance analysis in the 5G network is based on a standard configuration. This standard configuration includes 5G radio access technology, a 20 MHz bandwidth, FDD duplexing, and MIMO 2 × 2. Measurements primarily focus on the reverberation area of the chamber with horizontal antenna polarization, as this configuration demonstrates high performance.

### 1) THROUGHPUT

SHAP analysis determines the influence of each configuration on throughput, identifying the most significant contributors. As shown in Fig. 5, bandwidth and the

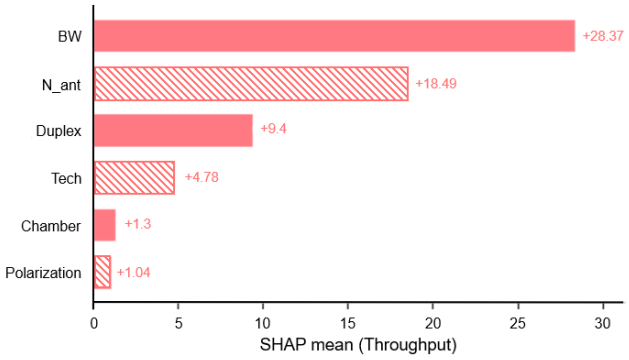



**FIGURE 5.** Importance of the configurations for the throughput via SHAP.

number of antennas are identified as the most significant variables, followed by the duplexing method and radio access technology. The chamber area and the polarization have a minor impact, subtly influencing measured throughput.

Fig. 5 also highlights variation in the CDF. The CDF differences among the configurations become less pronounced as the Shapley value is decreased. Fig. 6(a) presents CDFs for the three main configurations. Overall, throughput ranges between 41 and 192 Mbps. The maximum throughput is approximately 200 Mbps under standard configuration, aligning with the theoretical limit (see section III-B). The CDFs remain stable due to the controlled test environment, free from electromagnetic interference – an ideal setting for indoor applications requiring critical communications.

Throughput increases proportionally with bandwidth, as shown by the colored lines. The blue lines distinguish the contribution of duplexing and the number of antennas. The blue solid and dash-dot lines compare FDD and TDD, both using numerology $\mu = 0$ (15 KHz subcarrier spacing) [55]. FDD outperforms TDD, improving throughput by 26.32% on average. The blue solid and dotted lines compare SISO and MIMO ($2 \times 2$). Multi-antenna technologies improve throughput, provided the channel remains uncorrelated, as in multipath conditions.

Fig. 6(b) illustrates CDF comparisons for minor contributors. In this case, throughput variability remains between 169 and 194 Mbps. 5G NR technology increases throughput by 9.41% and stabilizes performance, reducing fluctuations. Meanwhile, the red and blue dash-dot lines compare measurements in semi-anechoic and semi-reverberant chamber areas. Differences are minimal, with slightly better results in LoS conditions. The purple and green dotted lines and red dash-dot lines show the effect of antenna polarization, which has a negligible impact, with a maximum improvement of 2.21%.

### 2) LATENCY

SHAP algorithm ranks the relevance of configurations according to latency, as shown in Fig. 7. The primary contributors are bandwidth and duplexing methods. Furthermore, antenna polarization, radio access technology, and the number of antennas have similar contributions to latency, while the chamber area has the least impact. At this point, given the low SHAP values for minor contributors, their influence on this KPI is expected to be minimal. Note that these values are derived from the complete dataset, making CDF benchmarking relevant, using the same standard configurations.

For clarity, the configurations are divided into two groups. Fig. 8(a) shows the CDFs for the main contributors mentioned and radio access technology. Fig. 8(b) focused on minor contributors: number of antennas, chamber area, and antenna polarization. Interpreting both, latency ranges from 6 to 19 ms.

In Fig. 8(a), solid lines compare differences in bandwidth, showing similar average latency values centered around 10.5 ms. The purple lines highlight other configurations. First, the purple solid and dash-dot lines compare duplexing methods, showing that FDD improves latency by 7.16% on average, though TDD provides more consistent results. Second, for certain configurations, NR outperforms LTE in latency. The purple solid and dotted lines compare these technologies, with LTE exhibiting 12.92% higher average latency a 33.87% degradation in the 90th percentile. This greater variability could be detrimental to synchronization-critical applications of URLLC.

Fig. 8(b) examines the lesser contributors to latency. As expected, these configurations offer minimal impact. However, minor differences are noted: multiple antennas introduce greater latency variability, visible in the solid lines. Similarly, the blue solid line, purple and green dash-dot lines indicate horizontal and vertical polarization cause higher variability, whereas pointing polarization remains stable. Finally, the blue solid and dotted lines show that multiple reflections in the reverberant chamber can reduce latency compared to LoS-only conditions, though the anechoic area offers more stable measurements. While these configurations do not significantly affect latency on average, they provide specific advantages depending on deployment conditions.

### 3) RELIABILITY

The reliability of the 5G network, in terms of lost packets, is assumed to be extremely high due to the short distances between Tx and Rx antennas relative to the communication frequencies. Consequently, the packet loss probability after connection establishment is practically zero. However, reliability can also be measured through retransmitted packets. As in previous cases, SHAP analysis is first applied (see Fig. 9). Unlike the previous ones, all configurations illustrate high SHAP values, indicating their relevance to the analysis.

Since all configurations impact reliability (see Fig. 9), the analysis is performed using CDFs, grouping configurations by relevance. Fig. 10(a) evaluates bandwidth, number of antennas, and duplexing method. In this case, reliability ranges from $3.194 \times 10^{-11}$ to $2.808 \times 10^{-10}$. The solid lines show bandwidth effects, with 20 MHz performing the best reliability. Compared to this baseline, 15 MHz, 10 MHz,

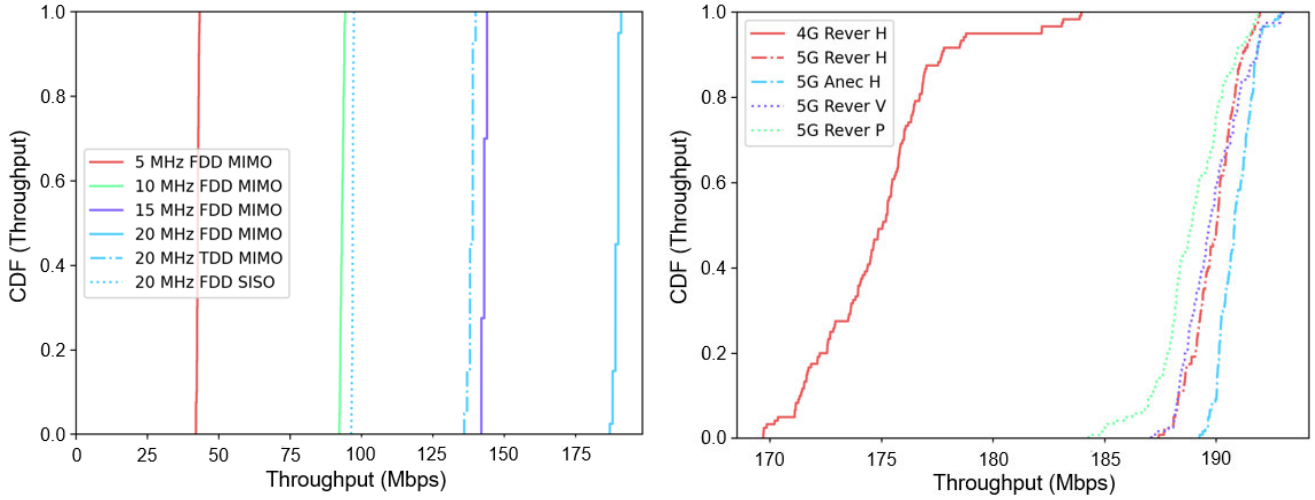



**FIGURE 6.** CDF of throughput in function of standard configuration. (a) In function of Bandwidth, number of antennas, and duplexing method. (b) In function of radio access technology, chamber zone, and antenna polarization.

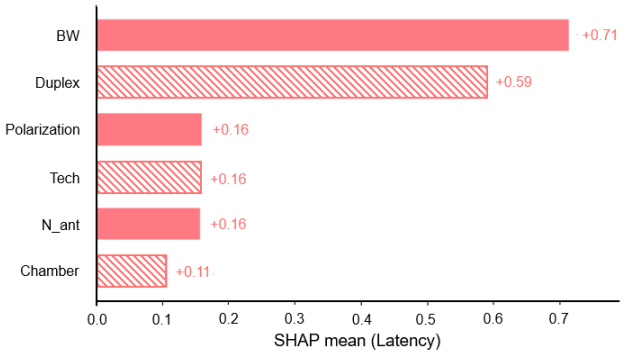



**FIGURE 7.** Importance of the configurations for the latency via SHAP.

and 5 MHz exhibit average degradation of 32.56%, 72.49%, and 196.50%, respectively. Despite handling more packets per time slot, increasing bandwidth enhances reliability and network stability. The red solid and dash-dot red lines compare FDD and TDD, showing a 40.73% reliability improvement with FDD. Meanwhile, the red solid and dotted red lines highlight the impact of multiple antennas. In this case, MIMO $2 \times 2$ improves reliability by 74.86% over SISO.

Fig. 10(b) examines radio access technology, chamber area, and antenna polarization, with reliability ranging from $3.194 \times 10^{-11}$ and $1.475 \times 10^{-10}$. The solid lines reveal that vertical and horizontal polarizations yield similar results, although vertical polarization shows a slight 5.76% improvement over horizontal and a significant 54.36% gain over pointing polarization. The blue solid and dash-dot blue lines compare NR and LTE, with 5G NR improving reliability by 29.37%. Finally, the blue solid and dotted lines represent the contribution of the chamber areas, where the reverberant area outperforms the anechoic area by 79.83%. This is attributed to the higher probability of successful packet transmission and reception in multipath environments.

**TABLE 4.** Experimental setups for performance comparison.

| Setup | BW | Duplex | N_ant | Chamber | Pol. |
|---|---|---|---|---|---|
| **Setup 1** | 20 MHz | FDD | MIMO | Rever | H |
| **Setup 2** | 20 MHz | FDD | MIMO | Anechoic | H |
| **Setup 3** | 20 MHz | FDD | SISO | Rever | H |
| **Setup 4** | 20 MHz | FDD | MIMO | Rever | V |

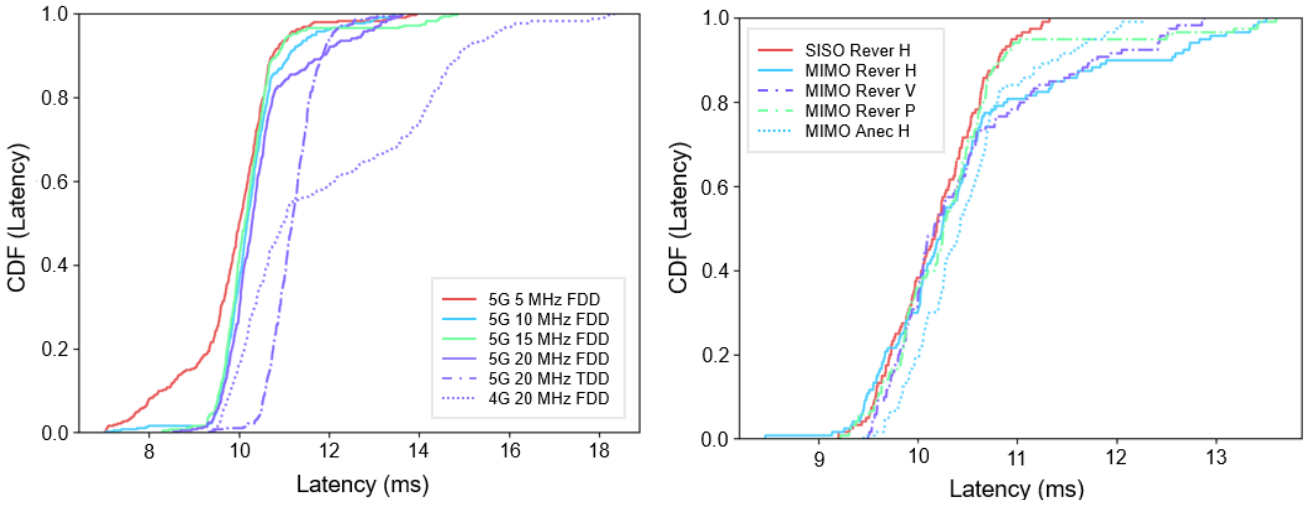
### C. STUDY OF EMBB AND URLLC USE CASES

This section studies ten use cases related to eMBB or URLLC services to determine optimal configuration combinations that satisfy QoS requirements. The objective is to identify the most suitable configurations for different service requirements, ensuring sufficient QoS for each use case.

#### 1) ANALYSIS OF ENHANCED CONFIGURATIONS

First, a performance comparison between the two radio access technologies (LTE and NR) is shown. While previous sections examined standard 5G configurations, this analysis considers four setups, as configuration-dependent variations may occur. For this purpose, the setups include: a balanced configuration (Setup 1), an enhanced throughput (Setup 2), an enhanced latency (Setup 3), and an enhanced reliability (Setup 4). Note that all configurations share a 20 MHz bandwidth and FDD. Table 4 summarizes these configurations.

The throughput comparison in Fig. 11(a) confirms that NR outperforms LTE in all setups. The 5G results remain consistent across setups, as most configurations have a minor impact on throughput, except Setup 3, which modifies the number of antennas. As expected, Setup 2 slightly improves throughput. Regarding LTE, throughput is comparable to NR under SISO but degrades significantly with MIMO. Furthermore, LTE exhibits greater throughput variability across configurations. For instance, performance in the anechoic




(a) (b)

**FIGURE 8.** CDF of latency in function of standard configuration. (a) In function of Bandwidth, duplexing method, and radio access technology. (b) In function of number of antennas, chamber zone, and antenna polarization.

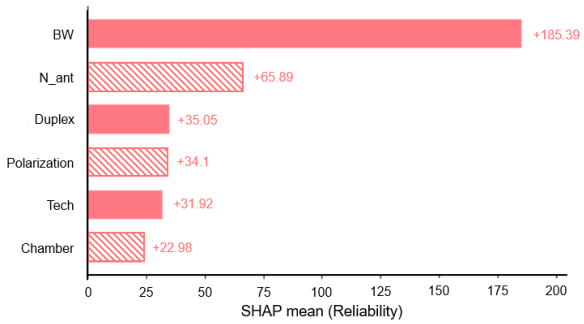



**FIGURE 9.** Importance of the configurations for the reliability using SHAP.

chamber (Setup 2) is worse, and antenna polarization has a significant impact (Setup 4). The setup considered as standard in the 5G analysis provides the best throughput for LTE.

Fig. 11(b) shows the latency comparison. The red boxes indicate that the case analyzed for 5G is unusual since it represents a significant improvement of NR over LTE. This demonstrates that 5G still achieves slightly lower latency. Notably, Setup 2 slightly worsens latency demonstrating that throughput and latency-enhanced setups are not strictly opposite, as confirmed by the PCA multivariate analysis.

Fig. 11(c) examines reliability based on retransmission rates. As expected, 5G generally improves reliability, except in Setup 2 –which uses SISO. Setup 4 provides higher reliability, as assumed. Interestingly, some setups have opposite effects across radio technologies. For instance, Setup 3 achieves the best retransmission rate in LTE but the worst in NR, likely due to physical layer differences in NR technologies.

### 2) STUDY OF SERVICE EMBB AND URLLC

Finally, Table 5 presents the study of eMBB and URLLC use cases. It lists ten use cases along with the QoS requirements defined by 3GPP in [19], [20], and [21] for throughput (T), end-to-end latency (L), and reliability (R). Additionally, it assigns an enhanced setup identified in this study that meets the requirements for each use case.

eMBB services are characterized by high data rates and low latency [19], supporting various interactive applications requiring high performance. These include cloud/edge/split rendering, gaming, training data exchange between AR/VR devices, and VR content consumption via tethered headsets. The QoS requirements for these applications include end-to-end latencies between 5 and 10 ms and user data rates of at least 100 Mbps, ensuring high reliability in both directions.

Augmented Reality (AR) [19] enhances real-world environments, demanding high data rates, low latency, and precise location accuracy. This use case includes video streaming, telepresence, and remote healthcare, with an end-to-end latency requirement of 100 ms. Additionally, streaming in crowded areas necessitates a latency below 20 ms.

For real-time interactive VR scenarios [19], motion-to-photon (MTP) delay significantly affects user experience. Reducing RTT below 25 ms is crucial for smooth image rendering within VR devices. Streaming VR applications [19], such as panoramic videos and live broadcasts, require 4K resolution transmissions with minimal rendering delay, ensuring end-to-end latencies below 25 ms.

Cloud gaming [19] shares similar QoS demands with VR, relying on cloud-based processing and rendering. This requires high data rates for graphical content and low latency for responsiveness. Interactive gaming demands latencies below 50 ms, with a minimum data rate of 100 Mbps for high-definition graphics.

According to Vehicle-to-Everything (V2X) communications, this study focuses on vehicle platooning, which includes cooperative driving, reporting, and information sharing between UEs and Roadside Units (RSUs) [20]. End-to-end latency requirements vary between 10 and 500 ms.

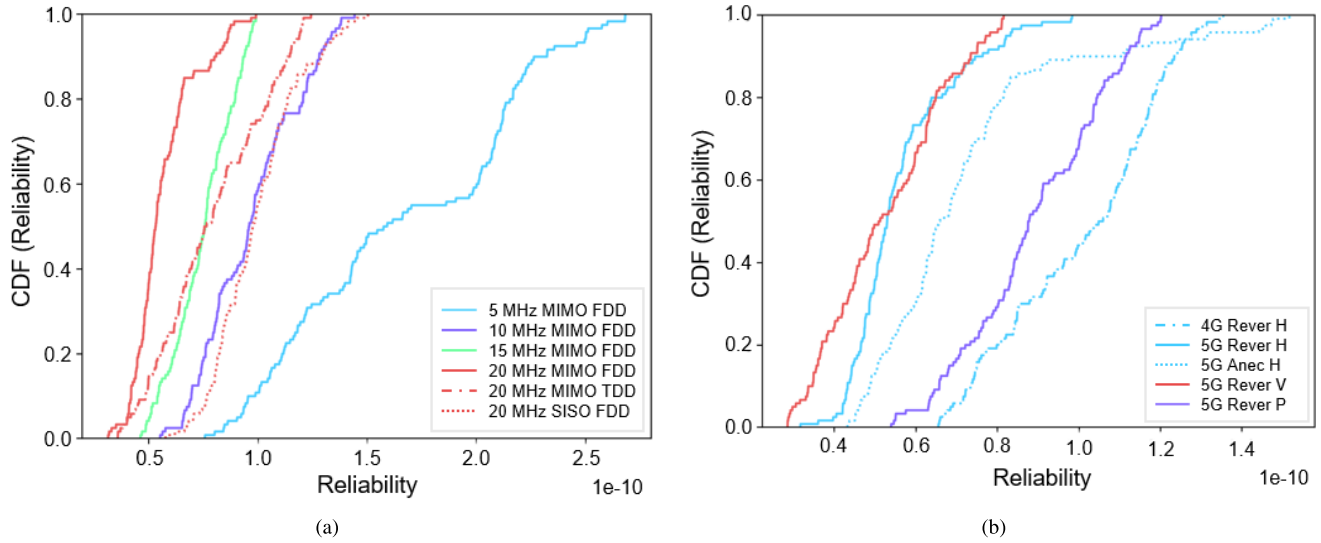



**FIGURE 10.** CDF of reliability in function of standard configuration. (a) In function of bandwidth, duplexing method, and number of antennas. (b) In function of radio access technology, chamber zone, and antenna polarization.

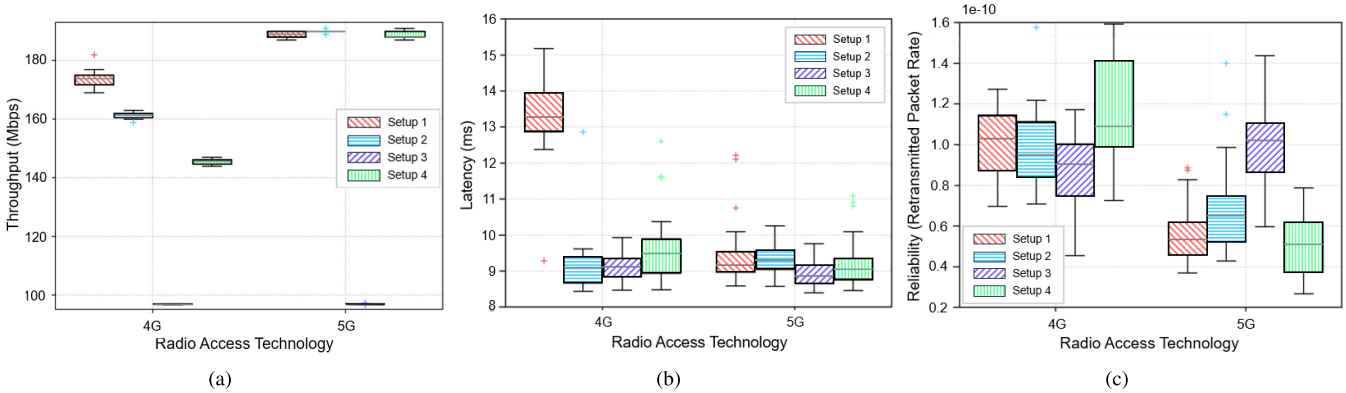



**FIGURE 11.** Comparison of LTE and NR based on defined setups. (a) As a function of throughput. (b) As a function of latency. (c) As a function of reliability.

The URLLC use cases focus on cyber-physical control applications in vertical domains. These typically demand low transmission rates, ranging from a few hundred Kbps to several tens of Mbps.

Control-to-control (C2C) communication [21] is widely used in industrial environments, where multiple controllers coordinate tasks such as newspaper printing or vehicle assembly. This requires synchronization and real-time data exchange with strictly low latencies.

Mobile robots and automated guided vehicles (AGVs) play a key role in industrial logistics, performing tasks like assisting in work steps and transporting goods. These use cases are categorized into five latency-sensitive applications [21]: (1) precise cooperative robotic motion control ($\leq$ 1 ms), (2) machine control (1 - 10 ms), (3) cooperative driving (10 - 50 ms), (4) video-operated remote control (10 - 100 ms), and (5) mobile robot operation and traffic management (40 - 500 ms).

Motion control [21] ensures precise movement of machine components by exchanging actuator commands and sensor feedback in a deterministic manner. Meanwhile process automation [21] involves deploying sensors for monitoring environment conditions, material inventory, and process status, transmitting data to controllers for decision-making.

Table 5 evaluates the feasibility of supporting these services. All setups demonstrate high reliability, ensuring the provision of both eMBB and URLLC services in controlled environments. However, the trade-off between throughput, latency, and reliability remains a fundamental challenge in 5G network deployments, as optimizing one metric often degrades another.

Throughput and reliability are inherently linked, yet excessive reliability mechanisms can introduce performance drawbacks. For instance, increasing Hybrid Automatic Repeat Request (HARQ) enhances reliability through error correction but simultaneously increases retransmissions, thereby reducing throughput. Similarly, latency and reliability exhibit an inverse-proportional relationship. While retransmission mechanisms improve reliability, they also increase delays. Conversely, minimizing retransmission to reduce latency may

**TABLE 5.** Study of eMBB and URLLC use cases [19], [20], [21].

| Services | Use Case | QoS Requirements | | | NR Configurations | | | | | | | | | | | |
|---|---|---|---|---|---|---|---|---|---|---|---|---|---|---|---|---|
| | | Throughput | Latency | Reliability | Setup 1 | | | Setup 2 | | | Setup 3 | | | Setup 4 | | |
| | | | | | T | L | R | T | L | R | T | L | R | T | L | R |
| eMBB | High Data Rate/Low Latency | $\geq$ 100 Mbps | 5-10 ms | $>$ 99,9% | ✓ | ✗ | ✓ | ✓ | ✗ | ✓ | ✗ | ✓ | ✓ | ✓ | ✗ | ✓ |
| | Augmented Reality | $\geq$ 100 Mbps | $\leq$ 80 ms | $>$ 99.999% | ✓ | ✓ | ✓ | ✓ | ✓ | ✓ | ✗ | ✓ | ✓ | ✓ | ✓ | ✓ |
| | Virtual Reality Interactive | $\geq$ 100 Mbps | $\leq$ 25 ms | $>$ 99.999% | ✓ | ✓ | ✓ | ✓ | ✓ | ✓ | ✗ | ✓ | ✓ | ✓ | ✓ | ✓ |
| | Virtual Reality Streaming | 16-50 Mbps | $\leq$ 25 ms | $>$ 99.999% | ✓ | ✓ | ✓ | ✓ | ✓ | ✓ | ✓ | ✓ | ✓ | ✓ | ✓ | ✓ |
| | Cloud Gaming | $\geq$ 100 Mbps | $\leq$ 50 ms | $>$ 99.999% | ✓ | ✓ | ✓ | ✓ | ✓ | ✓ | ✗ | ✓ | ✓ | ✓ | ✓ | ✓ |
| | V2X (Vehicle Platooning) | 50-65 Mbps | 10-500 ms | $>$ 99,9% | ✓ | ✗ | ✓ | ✓ | ✗ | ✓ | ✓ | ✓ | ✓ | ✓ | ✗ | ✓ |
| URLLC | C2C Communication | - | $\leq$ 5ms | $>$ 99.9999% | ✓ | ✗ | ✓ | ✓ | ✗ | ✓ | ✓ | ✗ | ✓ | ✓ | ✗ | ✓ |
| | Mobile Robots | $>$ 10 Mbps | 1-500 ms | $>$ 99.9999% | ✓ | ✗ | ✓ | ✓ | ✗ | ✓ | ✓ | ✗ | ✓ | ✓ | ✗ | ✓ |
| | Motion Control System | - | 1-2 ms | $>$ 99.9999% | ✓ | ✗ | ✓ | ✓ | ✗ | ✓ | ✓ | ✗ | ✓ | ✓ | ✗ | ✓ |
| | Process Automation | - | $>$ 10 ms | $>$ 99.9999% | ✓ | ✓ | ✓ | ✓ | ✓ | ✓ | ✓ | ✓ | ✓ | ✓ | ✓ | ✓ |

compromise reliability, leading to potential packet loss or degraded service quality.

MNOs must carefully consider reliability, particularly in outdoor deployment. Reliability can be significantly affected by obstructions, reflections, and dynamic environmental conditions. To mitigate these issues, retransmission mechanisms are required – an approach that, while enhancing reliability, inherently increases latency and constrains throughput.

Regardless of the environment, the primary challenge lies in managing the trade-off between throughput and latency. They also follow an inverse proportional relationship. For services without strict requirements in both metrics, Setups 1, 2, and 4 provide sufficient throughput and latencies well below the required thresholds. The main difficulty arises with latency-sensitive services such as V2X, which require stringent performance for both KPIs. In this case, only Setup 3 meets the latency requirements, although it offers lower throughput compared to the other configurations.

All eMBB services can be supported with the current setups. The only unmet requirements correspond to URLLC services with extremely low latency demands (e.g. C2C communication), which require latencies below 5 ms, unachievable with the current setups. Therefore, latency reduction is essential to support these services. Several challenges must be addressed to achieve lower latency. The following are key issues in URLLC and feasible techniques - at least theoretically - to mitigate them:

- **MAC Scheduling Complexity:** Reducing the complexity of MAC scheduling algorithms helps enable high-speed networks and lower latency. Configured grants can be used to pre-allocate resources to UEs, eliminating the need for resource requests before each transmission and thus reducing latency.
- **Control Overhead:** Minimizing control overhead in transmitted packets enhances latency efficiency, particularly in wireless networks. Grant-free access can be applied, allowing the system to skip the resource assignment procedure and reduce latency.
- **Shorter Transmission Time Interval (TTI):** Lowering TTI decreases latency in NR networks. This can be achieved by using higher numerologies in TDD systems or employing mini-slot configurations for faster transmissions.

However, these techniques require strict hardware and software specifications to meet latency targets. To our knowledge, some of these techniques (e.g. configured grants) are not yet available in commercial UE equipment.

It is also important to note that the analysis assumes isolated service deployment. In real scenarios, additional complexity arises when eMBB and URLLC services are deployed simultaneously. A key challenge in such cases is efficient packet scheduling, which involves transmitting packets from multiple services, even by interrupting ongoing transmissions (puncturing), through service prioritization. Typically, network slicing should be applied to differentiate services according to their QoS requirements and enable dedicated resource allocation per service or group of services with similar requirements.

## V. CONCLUSION AND FUTURE WORK

In this work, a private 5G network is implemented using the Amarisoft platform on general-purpose equipment. A series of experiments is conducted to evaluate three KPIs: throughput, latency, and reliability. These test campaigns took place in a semi-anechoic and semi-reverberant chamber, providing an electromagnetically controlled environment that isolates different propagation behaviors. This setup enabled a precise and reproducible study of how different configurations impact on network performance.

A comprehensive dataset is collected, representing the behavior of a real 5G deployment. The data is analyzed using multivariate and univariate methods, with PCA and SHAP as key tools. Principal Component Analysis demonstrates that throughput, latency, and reliability are not strictly opposing KPIs, meaning that fine-tuning the configurations allows for trade-offs between them. Meanwhile, the univariate analysis highlights how different configurations independently affect each KPI.

The analysis revealed several key findings. The maximum throughput achieved in our 5G networks is 193.08 Mbps, approaching the theoretical limit of our testbed due to our hardware equipment and software license. The minimum

latency observed is 6.82 ms, meeting the requirements for eMBB services but falling short of the extremely low-latency demands of URLLC. Furthermore, the networks exhibit extremely high reliability, highlighting their robustness in controlled environments.

This research further explores the feasibility of supporting different 5G service types (eMBB and URLLC). While the current setups are sufficient for eMBB, URLLC remains a major challenge that requires latencies under 5 ms. It provides an overview of these capabilities, emphasizing the trade-offs that exist between KPIs as well. From a practical standpoint, this study highlights valuable insights for mobile network operators (MNOs). Operators must carefully assess the service requirements and choose the appropriate configurations accordingly. This work presents 192 different configurations. The results also imply the need for advanced features and techniques in low-latency scenarios and multi-service environments, where eMBB and URLLC services must coexist.

Future research will focus on addressing the current latency limitations that prevent full compliance with URLLC requirements. Enhancing the physical and link layers configurations will be a key priority, particularly to reduce transmission delays in our testbed environment. Several latency reduction techniques will be explored as part of future implementation efforts: pre-allocating resources with configured grants, reducing control overhead, and using shorter TTI. Additionally, future lines of research will also examine the behavior of mixed-service deployments and the role of network slicing, puncturing, and dynamic scheduling algorithms in ensuring the coexistence of diverse 5G services with different QoS demands. This will bridge the gap between experimental lab results and real-world private network implementations, paving the way for more reliable and flexible 5G network solutions. Moreover, upcoming efforts will explore industrial applications, including Time Sensitive Networks (TSN) for deterministic communication, and multi-connectivity, where the UE simultaneously leverages multiple Wireless Access Technologies (WATs) – including 4G, 5G, Wi-Fi, and LiFi – to enhance overall performance and reliability.

## REFERENCES

[1] N. Jabagi, A. Park, and J. Kietzmann, "The 5G revolution: Expectations versus reality," *IT Prof.*, vol. 22, no. 6, pp. 8–15, Nov. 2020.

[2] N. H. Phuoc Dai, L. Ruiz, and R. Zoltan, "5G revolution: Challenges and opportunities," in *Proc. IEEE 21st Int. Symp. Comput. Intell. Informat. (CINTI)*, Budapest, Hungary, Nov. 2021, pp. 211–216.

[3] P. Pirinen, "A brief overview of 5G research activities," in *Proc. 1st Int. Conf. 5G Ubiquitous Connectivity*, Akaslompolo, Finland, Nov. 2014, pp. 17–22.

[4] *Minimum Requirements Related To Technical Performance for IMT2020 Radio Interface(s)*, document ITU-R M.2410, International Telecommunications Union, Nov. 2017.

[5] J. Orlosky, K. Kiyokawa, and H. Takemura, "Virtual and augmented reality on the 5G highway," *J. Inf. Process.*, vol. 25, pp. 133–141, 2017.

[6] X. Qiao, P. Ren, G. Nan, L. Liu, S. Dustdar, and J. Chen, "Mobile web augmented reality in 5G and beyond: Challenges, opportunities, and future directions," *China Commun.*, vol. 16, no. 9, pp. 141–154, Sep. 2019.

[7] Y. Siriwardhana, P. Porambage, M. Liyanage, and M. Ylianttila, "A survey on mobile augmented reality with 5G mobile edge computing: Architectures, applications, and technical aspects," *IEEE Commun. Surveys Tuts.*, vol. 23, no. 2, pp. 1160–1192, 2nd Quart., 2021.

[8] X. Wang, G. Han, X. Du, and J. J. P. C. Rodrigues, "Mobile cloud computing in 5G: Emerging trends, issues, and challenges [guest editorial]," *IEEE Netw.*, vol. 29, no. 2, pp. 4–5, Mar. 2015.

[9] P. Rost, C. J. Bernardos, A. D. Domenico, M. D. Girolamo, M. Lalam, A. Maeder, D. Sabella, and D. Wübben, "Cloud technologies for flexible 5G radio access networks," *IEEE Commun. Mag.*, vol. 52, no. 5, pp. 68–76, May 2014.

[10] N. Zhang, N. Cheng, A. T. Gamage, K. Zhang, J. W. Mark, and X. Shen, "Cloud assisted HetNets toward 5G wireless networks," *IEEE Commun. Mag.*, vol. 53, no. 6, pp. 59–65, Jun. 2015.

[11] A. Farooq, "Applications of digital holographic 3D video displays with 5G transmissions," *Sci. Technol. Innov. J.*, vol. 2, no. 2, p. 17, May 2021.

[12] A. El Essaili, S. Thorson, A. Jude, J. C. Ewert, N. Tyudina, H. Caltenco, L. Litwic, and B. Burman, "Holographic communication in 5G networks," *Ericsson Technol. Rev.*, vol. 2022, no. 5, pp. 2–11, May 2022.

[13] Y. N. Krishnan, C. N. Bhagwat, and A. P. Utpat, "Fog computing—Network based cloud computing," in *Proc. 2nd Int. Conf. Electron. Commun. Syst. (ICECS)*, Coimbatore, India, Feb. 2015, pp. 250–251.

[14] M. Attaran, "The impact of 5G on the evolution of intelligent automation and industry digitization," *J. Ambient Intell. Humanized Comput.*, vol. 14, no. 5, pp. 5977–5993, Feb. 2021.

[15] S. K. Rao and R. Prasad, "Impact of 5G technologies on Industry 4.0," *Wireless Pers. Commun.*, vol. 100, no. 1, pp. 145–159, Mar. 2018.

[16] G. Brown. (2019). *Ultra-Reliable Low-Latency 5G for Industrial Automation*. Qualcomm. Accessed: Mar. 3, 2024. [Online]. Available: https://www.qualcomm.com/content/dam/qcomm-martech/dm-assets/documents/ultra-reliable-low-latency-5g-for-industrial-automation.pdf

[17] M. I. Mamun, A. Rahman, M. A. Khaleque, M. F. Mridha, and M. A. Hamid, "Healthcare monitoring system inside self-driving smart car in 5G cellular network," in *Proc. IEEE 17th Int. Conf. Ind. Informat. (INDIN)*, vol. 1, Helsinki, Finland, Jul. 2019, pp. 1515–1520.

[18] H. Cao, S. Gangakhedkar, A. R. Ali, M. Gharba, and J. Eichinger, "A 5G V2X testbed for cooperative automated driving," in *Proc. IEEE Veh. Netw. Conf. (VNC)*, Columbus, OH, USA, Oct. 2016, pp. 1–4.

[19] *Speech and Multimedia Transmission Quality (STQ); QoS Parameters and Test Scenarios for Assessing Network Capabilities in 5G Performance Measurements*, document TR103.702 V1.1.1, 3GPP, Nov. 2020.

[20] *5G; Service Requirements for Enhanced V2X Scenarios*, document TS22.186 V17.0.0, 3GPP, Apr. 2022.

[21] *5G; Service Requirements for Cyber-Physical Control Applications in Vertical Domains*, document TS22.104 V16.5.0, 3GPP, Sep. 2020.

[22] *Amarisoft Products*. Amarisoft. Accessed: Nov. 23, 2024. [Online]. Available: https://www.amarisoft.com/

[23] M. Wen, Q. Li, K. J. Kim, D. López-Pérez, O. A. Dobre, H. V. Poor, P. Popovski, and T. A. Tsiftsis, "Private 5G networks: Concepts, architectures, and research landscape," *IEEE J. Sel. Topics Signal Process.*, vol. 16, no. 1, pp. 7–25, Jan. 2022.

[24] *Digital Cellular Telecommunications System (Phase 2+) (GSM); Universal Mobile Telecommunications System(UMTS); LTE; 5G; Release 16 Description; Summary of Rel-16 Work Items*, document TR21.916 V16.2.0, 3GPP, Jul. 2022.

[25] R. Tuninato, D. G. Riviello, R. Garello, B. Melis, and R. Fantini, "A comprehensive study on the synchronization procedure in 5G NR with 3GPP-compliant link-level simulator," *EURASIP J. Wireless Commun. Netw.*, vol. 2023, no. 1, p. 111, Oct. 2023.

[26] M. C. Lucas-Estañ and J. Gozalvez, "Sensing-based grant-free scheduling for ultra reliable low latency and deterministic beyond 5G networks," *IEEE Trans. Veh. Technol.*, vol. 71, no. 4, pp. 4171–4183, Apr. 2022.

[27] *Dataset Measurenments*. Wireless and Multimedia Networking Lab. Accessed: Apr. 29, 2025. [Online]. Available: https://github.com/felixdelgadoferro/Experimental5GNetworkPerformanceAnechoicChamber.git

[28] J. Camacho, A. Pérez-Villegas, R. A. Rodríguez-Gómez, and E. Jiménez-Mañas, "Multivariate exploratory data analysis (MEDA) toolbox for MATLAB," *Chemometric Intell. Lab. Syst.*, vol. 143, pp. 49–57, Apr. 2015.

[29] S. M. Lundberg and S.-I. Lee, "A unified approach to interpreting model predictions," in *Proc. 31st Conf. Neural Inf. Process. Syst. (NIPS)*, Long Beach, CA, USA, 2017, pp. 4768–4777.

[30] A. Ghosh, A. Maeder, M. Baker, and D. Chandramouli, "5G evolution: A view on 5G cellular technology beyond 3GPP release 15," *IEEE Access*, vol. 7, pp. 127639–127651, 2019.

[31] O. O. Erunkulu, A. M. Zungeru, C. K. Lebekwe, M. Mosalaosi, and J. M. Chuma, "5G mobile communication applications: A survey and comparison of use cases," *IEEE Access*, vol. 9, pp. 97251–97295, 2021.

[32] R.-G. Lazar, A.-V. Militaru, C.-F. Caruntu, C. Pascal, and C. Patachia-Sultanoiu, "Real-time data measurement methodology to evaluate the 5G network performance indicators," *IEEE Access*, vol. 11, pp. 43909–43924, 2023.

[33] E. O'Connell, D. Moore, and T. Newe, "Challenges associated with implementing 5G in manufacturing," *Telecom*, vol. 1, no. 1, pp. 48–67, Jun. 2020.

[34] M. I. Rochman, V. Sathya, D. Fernandez, N. Nunez, A. S. Ibrahim, W. Payne, and M. Ghosh, "A comprehensive analysis of the coverage and performance of 4G and 5G deployments," *Comput. Netw.*, vol. 237, Dec. 2023, Art. no. 110060.

[35] R. Pawlak, P. Krawiec, and J. Zurek, "On measuring electromagnetic fields in 5G technology," *IEEE Access*, vol. 7, pp. 29826–29835, 2019.

[36] J. Rischke, P. Sossalla, S. Itting, F. H. P. Fitzek, and M. Reisslein, "5G campus networks: A first measurement study," *IEEE Access*, vol. 9, pp. 121786–121803, 2021.

[37] M. Polese, L. Bonati, S. D'Oro, S. Basagni, and T. Melodia, "Understanding O-RAN: Architecture, interfaces, algorithms, security, and research challenges," *IEEE Commun. Surveys Tuts.*, vol. 25, no. 2, pp. 1376–1411, 2nd Quart., 2023.

[38] D. Xu, A. Zhou, X. Zhang, G. Wang, X. Liu, C. An, Y. Shi, L. Liu, and H. Ma, "Understanding operational 5G: A first measurement study on its coverage, performance and energy consumption," in *Proc. Annu. Conf. ACM Special Interest Group Data Commun. Appl., Technol., Architectures, Protocols Comput. Commun.*, Jul. 2020, pp. 479–494.

[39] H. Lim, J. Lee, J. Lee, S. D. Sathyanarayana, J. Kim, A. Nguyen, K. T. Kim, Y. Im, M. Chiang, D. Grunwald, K. Lee, and S. Ha, "An empirical study of 5G: Effect of edge on transport protocol and application performance," *IEEE Trans. Mobile Comput.*, vol. 23, no. 4, pp. 3172–3186, Apr. 2024.

[40] F. Moglie and V. M. Primiani, "Analysis of the independent positions of reverberation chamber stirrers as a function of their operating conditions," *IEEE Trans. Electromagn. Compat.*, vol. 53, no. 2, pp. 288–295, May 2011.

[41] J. D. Sanchez-Heredia, J. F. Valenzuela-Valdes, A. M. Martinez-Gonzalez, and D. A. Sanchez-Hernandez, "Emulation of MIMO Rician-fading environments with mode-stirred reverberation chambers," *IEEE Trans. Antennas Propag.*, vol. 59, no. 2, pp. 654–660, Feb. 2011.

[42] P.-S. Kildal, C. Orlenius, and J. Carlsson, "OTA testing in multipath of antennas and wireless devices with MIMO and OFDM," *Proc. IEEE*, vol. 100, no. 7, pp. 2145–2157, Jul. 2012.

[43] C. L. Holloway, H. A. Shah, R. J. Pirkl, W. F. Young, D. A. Hill, and J. Ladbury, "Reverberation chamber techniques for determining the radiation and total efficiency of antennas," *IEEE Trans. Antennas Propag.*, vol. 60, no. 4, pp. 1758–1770, Apr. 2012.

[44] X. Chen, J. Tang, T. Li, S. Zhu, Y. Ren, Z. Zhang, and A. Zhang, "Reverberation chambers for over-the-air tests: An overview of two decades of research," *IEEE Access*, vol. 6, pp. 49129–49143, 2018.

[45] A. Ramírez-Arroyo, A. Alex-Amor, C. García-García, Á. Palomares-Caballero, P. Padilla, and J. F. Valenzuela-Valdés, "Time-gating technique for recreating complex scenarios in 5G systems," *IEEE Access*, vol. 8, pp. 183583–183595, 2020.

[46] *5G; Management and Orchestration; 5G End to End Key Performance Indicators (KPI)*, document TS28.554, V16.6.0, Nov. 2020.

[47] M. I. Rochman, V. Sathya, N. Nunez, D. Fernandez, M. Ghosh, A. S. Ibrahim, and W. Payne, "A comparison study of cellular deployments in Chicago and Miami using apps on smartphones," 2021, *arXiv:2108.00453*.

[48] B. Cucor, P. Kamencay, M. Dado, and T. Petrov, "Experimental comparison of 4G and 5G technologies for connected and automated vehicles," in *Proc. 33rd Int. Conf. Radioelektronika*, Pardubice, Czech Republic, Apr. 2023, pp. 1–5.

[49] M. I. Rochman, V. Sathya, and M. Ghosh, "Outdoor-to-indoor performance analysis of a commercial deployment of 5G mmWave," in *Proc. IEEE Future Netw. World Forum (FNWF)*, Montreal, QC, Canada, Oct. 2022, pp. 519–525.

[50] B. S. Khan, S. Jangsher, A. Ahmed, and A. Al-Dweik, "URLLC and eMBB in 5G industrial IoT: A survey," *IEEE Open J. Commun. Soc.*, vol. 3, pp. 1134–1163, 2022.

[51] M. C. Lucas-Estañ, B. Coll-Perales, T. Shimizu, J. Gozalvez, T. Higuchi, S. Avedisov, O. Altintas, and M. Sepulcre, "An analytical latency model and evaluation of the capacity of 5G NR to support V2X services using V2N2V communications," *IEEE Trans. Veh. Technol.*, vol. 72, no. 2, pp. 2293–2306, Feb. 2023.

[52] A. P. K. Reddy, M. S. Kumari, V. Dhanwani, A. K. Bachkaniwala, N. Kumar, K. Vasudevan, S. Selvaganapathy, S. K. Devar, P. Rathod, and V. B. James, "5G new radio key performance indicators evaluation for IMT-2020 radio interface technology," *IEEE Access*, vol. 9, pp. 112290–112311, 2021.

[53] G. Soós, D. Ficzere, P. Varga, and Z. Szalay, "Practical 5G KPI measurement results on a non-standalone architecture," in *Proc. IEEE/IFIP Netw. Operations Manage. Symp.*, Budapest, Hungary, Apr. 2020, pp. 1–5.

[54] *Evolved Universal Terrestrial Radio Access (E-UTRAN); LTE; LTE Physical; General Description*, document TS36.201, V13.1.0, Apr. 2016.

[55] *5G; NR; Physical Layer Procedures for Data*, document TS38.214, V15.9.0, 3GPP, Apr. 2020.

[56] Y. Qu, G. Ostrouchov, N. Samatova, and A. Geist, "Principal component analysis for dimension reduction in massive distributed data sets," in *Proc. 2nd IEEE Int. Conf. Data Mining (ICDM)*, Maebashi, Japan, Apr. 2002, pp. 1984–1988.

[57] E. Saccenti and J. Camacho, "On the use of the observation-wise k-fold operation in PCA cross-validation," *J. Chemometrics*, vol. 29, no. 8, pp. 467–478, Jul. 2015.

[58] J. Camacho, "Observation-based missing data methods for exploratory data analysis to unveil the connection between observations and variables in latent subspace models," *J. Chemometrics*, vol. 25, no. 11, pp. 592–600, Nov. 2011.

[59] J. Camacho, A. Pérez-Villegas, P. García-Teodoro, and G. Maciá-Fernández, "PCA-based multivariate statistical network monitoring for anomaly detection," *Comput. Secur.*, vol. 59, pp. 118–137, Jun. 2016.

[60] M. Ribeiro, S. Singh, and C. Guestrin, "'Why should I trust you?' Explaining the predictions of any classifier," in *Proc. Conf. North Amer. Chapter Assoc. Comput. Linguistics, Demonstrations (NAACL)*, San Diego, CA, USA, 2016, pp. 1135–1144.

[61] J. C. Vesga, G. G. Acu, and J. E. S. Carrillo, "The value of Shapley as a strategy for resource optimization on power line communication (PLC)," *Ingenieria y Ciencia*, vol. 11, no. 22, pp. 189–211, Aug. 2015.



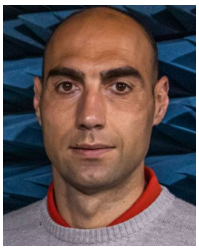
**FELIX DELGADO-FERRO** received the B.Sc. and M.Sc. degrees in telecommunication engineering from the University of Granada, Spain, in 2020 and 2022, respectively, where he is currently pursuing the Ph.D. degree in telecommunication engineering with the Wireless and Multimedia Networking Laboratory (WiMuNet), Department of Signal Theory, Telematics, and Communications. In 2023, he was a Visiting Doctoral Student with the Simula Research Laboratory (SINLab), University of Oslo, Norway. His current research interests include multipath protocols, heterogeneous networks, and optimization techniques for the IoT, 5G, and 6G networks.



**ALEJANDRO RAMÍREZ-ARROYO** was born in Córdoba, Spain, in 1997. He received the B.Sc., M.Sc., and Ph.D. degrees in telecommunication engineering from the University of Granada (UGR), Spain, in 2019, 2021, and 2023, respectively. From 2019 to 2024, he was with the Smart Wireless Applications and Technologies (SWAT) Research Group, Department of Signal Theory, Telematics, and Communications, University of Granada. In 2022, he was with the Wireless Communication Networks Section, Aalborg University (AAU), Denmark, as an Invited Ph.D. Student. Since 2024, he has been a Postdoctoral Researcher with the Department of Electronic Systems, AAU. His current research interests include optimization techniques, radio propagation, and channel characterization for mmWaves and 5G communications.



**JORGE NAVARRO-ORTIZ** received the M.Sc.E.E. degree from the University of Malaga, Spain, in 2001, and the Ph.D. degree from the University of Granada, in 2010. Then, he was with Nokia Networks, Optimi/Ericsson, and Siemens. He was an Assistant Professor with the University of Granada, in 2006. He is currently an Associate Professor with the Department of Signal Theory, Telematics and Communications, University of Granada. His research interests include wireless technologies for the IoT, such as LoRaWAN and 5G.



**JUAN F. VALENZUELA-VALDÉS** was born in Marbella, Spain. He received the degree in telecommunication engineering from the Universidad de Malaga, Malaga, Spain, in 2003, and the Ph.D. degree from the Universidad Politecnica de Cartagena, Cartagena, Spain, in 2008. He joined the Department of Information Technologies and Communications, Universidad Politecnica de Cartagena, in 2004. In 2007, he joined EMITE Ing., Murcia, Spain, as the Head of Research. In 2011, he joined the Universidad de Extremadura, Merida, Spain. In 2015, he joined the Universidad de Granada, Granada, Spain, where he is currently a Full Professor. He is also the Head of the SWAT Research Group, University of Granada; and the Co-Head of the Singular Laboratory of Electromagnetic Characterization of Microwave and Millimeter Devices and Antennas. His publication record comprised more than 100 publications, including 50 journal citation reports (JCR)-indexed articles and seven book chapters. He holds several national and international patents. His current research interests include wireless communications, radio frequency devices, antennas, and propagation. He received several prizes, including the National Prize for the Best Ph.D. Thesis in mobile communications by Vodafone.